Spectroscopic Properties of the States of Pig Pancreatic Phospholipase A_2 at Interfaces and Their Possible Molecular Origin†

Mahendra Kumar Jain*,‡ and Badri P. Maliwal*,‡,§

Department of Chemistry and Biochemistry, University of Delaware, Newark, Delaware 19716, and Center for Fluorescence Spectroscopy, Department of Biological Chemistry, University of Maryland Medical School, Baltimore, Maryland 21201

Received April 27, 1993; Revised Manuscript Received August 10, 1993®

ABSTRACT: The near-UV absorption and fluorescence spectroscopic properties of Trp-3 of pig pancreatic phospholipase A_2 (PLA2) in aqueous solution (E form) or at the interface without (E* form) or with a ligand at the active site (E*L form) are characterized. In the E form, the single tryptophan residue is exposed on the protein surface to the aqueous environment, as it is freely accessible to aqueous quenchers such as succinimide and acrylamide. The fluorescence quantum yield of E is about one-third that of *N*-acetyltryptophanamide, indicating significant intramolecular quenching processes including charge-transfer reactions, as seen by the D_2O effect. Upon binding of PLA2 to micelles of 1-hexadecylpropanediol-3-phosphocholine (E*), a positive difference spectrum with a shoulder at 284 nm ($\Delta\epsilon$ = 370 M^{-1} cm^{-1}) is observed. Similar difference spectra are also observed upon binding of sulfate ion to the E form. The fluorescence emission of E* is blue-shifted by about 10 nm to 336 nm, with a 2-fold higher quantum yield. Trp-3 in E* is significantly shielded from aqueous quenchers, and the D_2O effect on the quantum yield is still present. The UV difference spectrum for the E*-to-E*L transition is of large amplitude with peaks at 292 ($\Delta\epsilon$ = 2540 M^{-1} cm^{-1}) and 284 nm ($\Delta\epsilon$ = 2100 M^{-1} cm^{-1}), which suggests transfer of tryptophan from an aqueous to a less polar environment. Upon conversion to the E*L form, there is a further blue shift to 333 nm, with about a 20% increase in the fluorescence quantum yield. The frequency domain fluorescence intensity decays of Trp-3 in all three forms of the enzyme are complex and require up to four fluorescence lifetime components of about 0.1–0.3, 0.6–1.5, 2.3–3.2, and 6–7.5 ns. A significant shift in the population from the two short-lived components to the 3.2-ns component seems to account for the higher quantum yield on the E-to-E* change. The frequency domain anisotropy decays indicate a highly hindered Trp-3 in the E form whose limited motional freedom is lost upon the transition to E* and E*L forms. Compared to that in E*, Trp-3 in E*L is only marginally more shielded from the solvent. Most of the decrease in the accessibility of Trp-3 to the bulk aqueous phase occurs during the change from E to E*, while the dehydration of the enzyme–lipid microinterface occurs primarily during the E*-to-E*L transition. In conclusion, the spectral changes in the E-to-E* step are due to changes in the ionic environment of Trp-3 resulting from dampened segmental motions of the interfacial binding region, while the changes in the E*-to-E*L step are primarily due to the dehydration of the enzyme–lipid microinterface.

The kinetics of interfacial catalysis by secreted phospholipase A_2 (PLA2[1]) is quantitatively described by a modified Michaelis–Menten scheme (Jain & Berg, 1989; Berg et al., 1991) in which, as a pre-steady-state step, the enzyme in the aqueous phase (E) binds to the interface (E*):

$$E \overset{K_D}{\rightleftarrows} E^* + L \overset{K_L^*}{\rightleftarrows} E^*L$$

The E-to-E* step determines the overall steady-state concentration of the catalytically active enzyme in the interface. The enzyme at the interface can bind active-site-directed ligands (L) such as substrate, products of hydrolysis, or competitive inhibitor. Since interaction of E* with the substrate and the chemical step lead to processive hydrolysis at the interface, the E-to-E* equilibrium is important both for understanding the pre-steady-state kinetics (Jain et al., 1988), processivity of interfacial catalysis in the scooting and hopping modes (Jain & Berg, 1989; Berg et al., 1991), and interfacial activation (Jain et al., 1993) and for elaborating the structural features of PLA2 at the interface. This two-step formalism of interfacial catalysis implies a topological and temporal distinction between the binding of the enzyme to the interface and the catalysis at the interface, i.e., the binding of the enzyme to the interface is a prelude for catalysis; however, steps of the catalytic turnover cycle are not required for the binding of the enzyme to the interface (Verheij et al., 1981; Volwerk & de Haas, 1982; Jain & Berg, 1989).

Several functional features are apparent from the X-ray crystal structure of the PLA2 from several sources without or with an active-site-directed ligand (Dijkstra et al., 1981, 1983; Scott et al., 1990; Thunnissen et al., 1990; Noel et al., 1991; Tomoo et al., 1992). The catalytic site residue His-48 is localized in a cavity, the wall of which is lined with hydrophobic residues. The outside edge of this cavity is remarkably flat and includes some of the N-terminus residues

† This work was supported by PHS GM29703 to M.K.J. We thank Dr. J. R. Lakowicz for allowing the use of the facilities at the Center for Fluorescence Spectroscopy, supported by NSF DIR-8710401 and NIH RR-08119.

* Corresponding authors.
‡ University of Delaware.
§ University of Maryland.

® Abstract published in *Advance ACS Abstracts,* October 1, 1993.

[1] Abbreviations: deoxy-LPC, 1-hexadecylpropanediol-3-phosphocholine; DMPM, dimyristoyl-glycero-*sn*-3-phosphomethanol; DTPM, ditetradecyl-glycero-*sn*-3-phosphomethanol; 2H-GPC, 2-hexadecyl-*rac*-glycero-3-phosphocholine; Me-PLA, PLA2 methylated at His-48; MJ33, 1-hexadecyl-3-trifluoroethyl-*rac*-glycero-2-phosphomethanol; MJ72, 1-octyl-3-trifluoroethyl-*rac*-glycero-2-phosphomethanol; NATA, *N*-acetyltryptophanamide; Oct-PLA, PLA2 alkylated with 1-bromooctan-2-one at His-48; PLA2, phospholipase A_2 from pig pancreas unless stated otherwise.

0006-2960/93/0432-11838$04.00/0

including Trp-3 and several cationic residues. The role played by the residues forming this collar including Trp-3 in the binding of the enzyme to the interface has been explored by a variety of techniques (Verheij et al., 1981; Volwerk & de Haas, 1982; Ramirez & Jain, 1991). Binding of PLA2 to micelles results in a large amplitude difference absorbance spectrum with a peak at 292 nm, a shoulder at 284 nm, and a negative trough around 250 nm (Van Dam-Mieras et al., 1975; Hille et al., 1981, 1983; Dupureur et al., 1992a). Similarly, a significant blue shift and an enhancement in the fluorescence emission of Trp-3 (Van Dam-Mieras et al., 1975; Jain et al., 1982, 1986b; Dupureur et al., 1992a,b) and shielding from aqueous quenchers (Jain & Maliwal, 1985; Jain & Vaz, 1987; Ludescher et al., 1985) indicate that Trp-3 moves from a solvent accessible aqueous environment to a less polar environment in the micelle complex. The time-resolved fluorescence studies indicate complex photophysics (Jain et al., 1986b; Ludescher et al., 1985; Alcala et al., 1987; Kuipers et al., 1991) suggestive of the existence of both discrete and an interconverting quasicontinuum of enzyme conformers. Even though Trp-3 is exposed on the surface of the enzyme, the time-resolved anisotropy measurements indicate it to be significantly hindered in the E form, and it is essentially immobile in the enzyme bound to micelles of hexadecylphosphocholine (Ludescher et al., 1988; Kuipers et al., 1991). These results and molecular dynamics calculations (Sessions et al., 1988; Gros et al., 1990) indicate that the N-terminal region is rather rigid, most likely due to the extensive H-bonding network. Desolvation of the active site (Van Scharrenburg et al., 1985) and the enzyme–bilayer microinterface (Jain & Vaz, 1987) is also observed upon binding of an active-site-directed ligand to the enzyme at the interface.

A major limitation of virtually all biophysical studies reported so far is that a distinction between E and E*L forms of the enzyme has not been made.* Obviously, to understand the structural basis of interfacial catalysis, it is important to distinguish the E, E*, and E*L forms. These forms of PLA2 can now be distinguished in dispersions of a "neutral diluent" (Jain et al., 1991a,c). It may be recalled that PLA2 binds to aqueous dispersions of a neutral diluent, and the equilibrium is determined by the bulk concentration of the neutral diluent. Because of the low affinity of a neutral diluent molecule for the enzyme at the interface ($K_L^* > 2$ mol fraction), even at the maximum possible mole fraction (1) of the neutral diluent at the interface, the bound enzyme is predominantly in the E* form, i.e., the neutral diluent provides a noninteracting interface. On the other hand, active-site-directed ligands bind with high affinity to the E* form of the enzyme. Thus the E* + L-to-E*L equilibrium depends on the intrinsic affinity of the enzyme for such ligands codispersed in micelles of the neutral diluent. With a suitable choice of the neutral diluent and the ligand, it is possible to control the proportion of and thus to characterize the E* and E*L forms of PLA2. In this paper we have used this strategy to characterize the fluorescence and near-UV absorbance properties of E, E*, and E*L forms of PLA2. As elaborated in the Discussion, these results facilitate an understanding of the functional, topological, and temporal properties of PLA2 at the interface in the E* and E*L forms.

MATERIALS AND METHODS

Methods for the preparation of native (PLA2) and alkylated (Me-PLA and Oct-PLA) PLA2 (Jain et al., 1991b), phospholipids (Jain et al., 1986a), competitive inhibitors MJ33 and MJ72 (Jain et al., 1991c), and neutral diluents deoxy-LPC and 2H-GPC (Jain et al., 1991a,c) have been described. All other reagents, proteins, and phospholipids used here were of better than 99% purity, ascertained by thin-layer chromatography or HPLC. Unless stated otherwise, all protection measurements were made in 10 mM Tris, 0.5 mM $CaCl_2$ at pH 8.0 and 23 °C. Typically >2 mM deoxy-LPC was used as a neutral diluent; however, some measurements were also carried out with 2H-GPC. Under these conditions, virtually all PLA2 is in the E* form (Jain et al., 1991a,c).

The experimental protocols for the determination of interfacial equilibrium dissociation constants for the active-site-directed ligands (K_L^*) have been described in detail in earlier publications as noted. Kinetics of modification of PLA2 by *p*-nitrophenacyl bromide (Sigma) was monitored (Jain et al., 1991a) in the presence of appropriate neutral diluent and active-site-directed ligands. Steady-state fluorescence measurements were made on a SLM 4000 or 4800S spectrophotometer with a 450-W xenon lamp as the source. Unless stated otherwise, the excitation wavelength was 292 nm for the steady-state fluorescence intensity measurements (Jain et al., 1986b). For steady-state fluorescence measurements, the protein concentration was kept at 3–10 μM in the buffer containing 3 mM $CaCl_2$ with no noticeable inner-filter effects.

For quenching experiments, aliquots of freshly prepared 2.5 M stock solutions of the quencher, succinimide (Sigma) or acrylamide (Sigma), were added to stirred 1.5-mL samples of 4 μM PLA2 in the buffer containing other appropriate reagents. The measured intensities at 292 nm were corrected for dilution effects. Since the quencher concentration was kept below 0.6 M, corrections from the absorbance of the quencher were less than 5%. The plot of $(F_0/F - 1)$ versus the quencher concentration was linear with correlation coefficients > 0.98. The slopes of such plots provided the Stern–Volmer constants, $K_{SV} = k_q\langle\tau\rangle$, where k_q is the collisional rate constant and $\langle\tau\rangle$ is the average fluorescence lifetime.

The ultraviolet absorption spectra were obtained on a HP8452A spectrophotometer equipped with a diode array detector with a resolution of 2 nm. Typically the protein concentration was kept at 20 μM and the concentration of the neutral diluent at 3.3 mM. The calculations for the difference spectra and corrections for the scattering changes were carried out with the standard software provided by the manufacturer (Hewlett-Packard).

Fluorescence decay measurements were performed using the 10-GHz frequency domain fluorometer as described elsewhere (Laczko et al., 1990). The output of the harmonic content of a rhodamine 6G dye laser, synchronously pumped with a mode-locked argon ion laser, cavity-dumped at 3.75 MHz, and frequency-doubled to 295 or 298 nm was used as the excitation source. The dynamic fluorescence measurements were made in 4-mm-path length cuvettes with 60 μM PLA2. The emission was observed through a broad emission window obtained by use of a combination of Corning 0–54 and 7–54 filters. The frequency responses of the emission intensity decays were analyzed as a sum of exponentials by nonlinear least-squares fitting routines (Lakowicz et al., 1984):

$$I(t) = \sum_i \alpha_i e^{-t/\tau_i}$$

where α_i and τ_i are, respectively, the amplitudes and the associated fluorescence lifetime components. The average

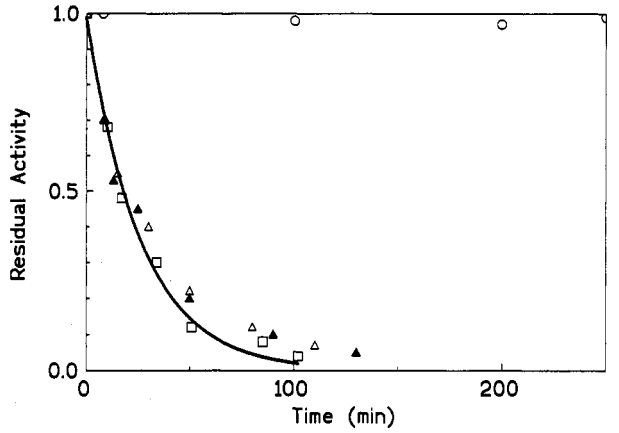

FIGURE 1: Time course of inactivation of PLA2 (30 μM) by alkylation by *p*-nitrophenacyl bromide (1 mM) (□) in the aqueous phase, (△) in 3.3 mM deoxy-LPC, (▲) in 3.3 mM 2H-GPC, and (○) in 0.5 mM products of hydrolysis of DMPM. The reaction mixture also contained 0.5 mM $CaCl_2$ and 50 mM NaCl in 50 mM cacodylate buffer at pH 7.3 and 23 °C.

fluorescence lifetime $\langle\tau\rangle$ was computed as:

$$\langle\tau\rangle = \sum \alpha_i\tau_i$$

The anisotropy decays $r(t)$ were analyzed as a sum of exponentials as follows (Weber, 1977; Maliwal & Lakowicz, 1986):

$$r(t) = \sum_i r_i\, e^{-t/\theta_i}$$

where θ_i are the rotational correlation times and r_i are associated anisotropies. The sum of preexponentials, Σr_i, gives the zero-time or limiting anisotropy r_0.

RESULTS

Alkylation of PLA2. The rate of alkylation of the catalytic site residue, His-48, as measured by the inactivation of PLA2 (Jain et al., 1991a) is shown in Figure 1. The half-times for alkylation of PLA2 in the aqueous phase and in the presence of deoxy-LPC and 2H-GPC were 18 (fitted to the smooth curve), 21, and 19 min, respectively. This suggests that the enzyme in the aqueous solution is inactivated by *p*-nitrophenacyl bromide at virtually the same rate as it is in the presence of the two neutral diluents, where all of the enzyme is in the E* form. On the other hand, as is also shown in this figure, in the presence of the products of hydrolysis the half-time for alkylation was well over 1200 min. These results, therefore, show that only the E or E* forms of the enzyme, but not the E*L form, is alkylated. Similar behavior was observed in the presence of other active-site-directed ligands (Jain et al., 1991a,c; Dupureur et al., 1992a,b). From the half-time for alkylation observed in the presence of a ligand it is possible to calculate the value of the equilibrium dissociation constant, K_L^* (Jain et al., 1991a), which is related to the fraction of the enzyme in the E*L form as

$$f_b = \frac{E^*L}{E^* + E^*L} = \frac{X_L}{X_L + K_L^*}$$

Based on the results shown in Figure 1, the K_L^* value for the two neutral diluents is >3 mol fraction, i.e., more than 75% of the enzyme is in the E* form at the interface of the neutral diluent alone. This is a lower limit estimate; the actual value is >90% (Jain et al., 1991a,c). Similarly, from the value of the dissociation constant for the products of hydrolysis, $K_L^* = K_P^* = 0.025$ mol fraction (Jain et al., 1991a), under the experimental conditions in Figure 1 where $X_P = 1$ mole fraction, more than 97% of the enzyme at the interface would be in the E*P form. It may be noted that even in the presence of subsaturating concentrations of the neutral diluent, the presence of a ligand of a significantly higher affinity would effectively shift the equilibrium from E to E* to E*L.

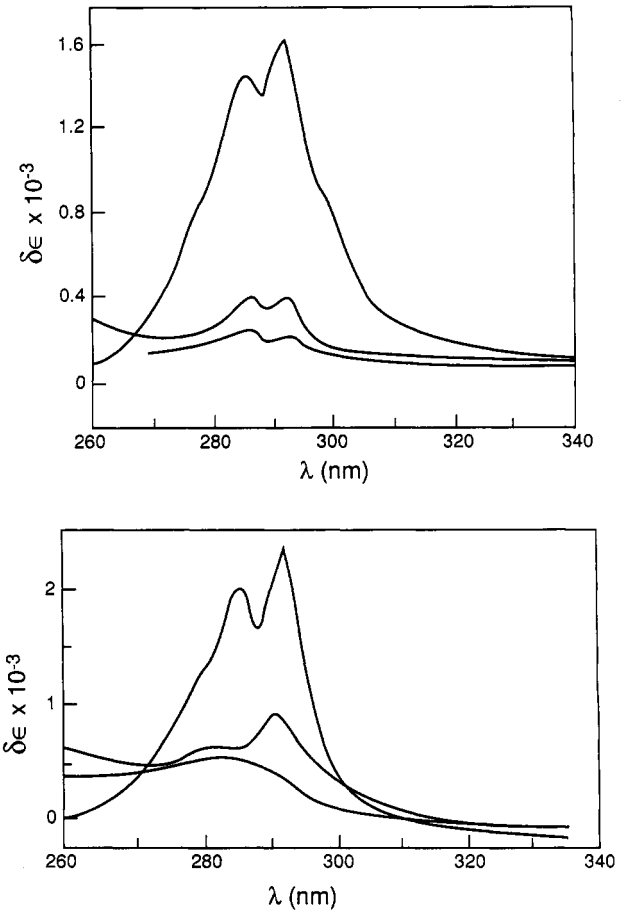

FIGURE 2: (Top) UV-difference spectra for PLA2 on binding (from top) to vesicles of the products of hydrolysis (0.5 mM), to 3.3 mM deoxy-LPC, and to 3.3 mM 2H-GPC. The reaction mixture also contained 20 mM Tris, 3 mM $CaCl_2$, and 10 mM NaCl at pH 8.0 and 23 °C. The spectra were corrected for the turbidity change. (Bottom) UV-difference spectra (from top) for PLA2, Me-PLA, and Oct-PLA in 3.3 mM deoxy-LPC induced on the addition of 0.1 mM MJ33.

UV Absorbance Characteristics of the E and E*L Forms.* As shown in Figure 2 (top), upon binding of PLA2 to micelles of a neutral diluent (2H-GPC), an unstructured positive difference spectrum was observed with a shoulder at 284 nm ($\Delta\epsilon < 500\ M^{-1}\ cm^{-1}$). In the difference spectrum for E* on a deoxy-LPC micelle, besides the shoulder at 284 nm, a small peak at 288 nm was observed. As implied by the protection results (Figure 1) and as elaborated next, it is unlikely that this feature is from a small (<20%) population of the E*L due to a weak affinity of deoxy-LPC for the active site of PLA2.

There is considerable uncertainty in the exact shape of the UV difference spectrum because of the small amplitude of the changes during the E-to-E* change. Also, significant corrections for the scattering were required due to a change in the size of the micelles on the binding of the enzyme. In any case, the shape of the spectrum, the magnitude of the overall change, and a modest red shift is unlike that seen when a tryptophan moves into a less polar environment (Donovan, 1969).

Absorbance Changes Associated with the Occupancy of the Active Site at the Interface. A significantly different UV

Table I: Absorbance and Fluorescence Characteristics of E, E*, and E*L Forms of PLA2

property	E	E* [a]	E*·MJ33	E*P
$\Delta\epsilon$ at 292 nm (M^{-1} cm^{-1})		250	2540	2280
$\Delta\epsilon$ (292/284)		0.27	1.20	1.16
λ_{max} (nm) (emission)	345	336	333	333
RQY in H_2O	1	2.1	2.52	2.44
RQY in D_2O	1.18	2.25	2.56	2.4
$\langle\tau\rangle$ (ns)	1.10	2.04	2.02	2.36
$k_q \times 10^9$ (succinamide)	4.5	0.25	<0.1	<0.2
$k_q \times 10^9$ (acrylamide)	6.5	1.25	0.4	0.6

[a] These values are at 3 mM calcium. The relative quantum yields are corrected for the change in the absorbance. The deoxy-LPC concentration was 3.3 mM, and that of the active-site-directed ligand (MJ33) was 0.3 mM. RQY, relative quantum yield.

absorption difference spectrum was obtained for the E*-to-E*L change induced by the titration of the mixture of PLA2 and the neutral diluent with an active-site-directed amphiphile, the products of hydrolysis. As shown in Figure 2 (top) and summarized in Table I, this difference spectrum is characterized by peaks at 292 ($\Delta\epsilon$ = 2540 M^{-1} cm^{-1}) and 284 ($\Delta\epsilon$ = 2120 M^{-1} cm^{-1}), a shoulder at near 300, and a small negative trough near 260 nm. The amplitude at 292 nm depends on the mole fraction of MJ33 and reaches a maximum value at saturating mole fractions. Both the amplitude and the shape of the difference spectrum for the E*-to-E*L change are similar to those observed with the transfer of a tryptophan residue to a less polar environment (Donovan, 1969). The difference spectra characteristic of the E*-to-E*L change were also obtained with several competitive inhibitors, substrate analogues, and the products of hydrolysis, which suggested that the microenvironments of Trp-3 in E*L, E*S, and E*P are similar [results not shown; see, however, Dupureur et al. (1992a)]. Taken together, these difference spectra (Figure 2) suggest that the microenvironment of Trp-3 is only slightly less polar in the E* form than in the E form, but it is significantly less polar in the E*L form.

The difference spectra for E*L obtained with the native and the His-48-modified Me-PLA2 and Oct-PLA2 in the presence of active-site-directed inhibitor are shown in Figure 2 (bottom). The difference spectrum with the native enzyme is similar to that obtained with the products of hydrolysis; however, only a small peak was observed with the alkylated enzymes and the overall spectra are similar to those obtained for the E-to-E* transition. As expected, the characteristic E*-to-E*L difference spectrum with the native enzyme was not observed in the absence of calcium (results not shown), which is an essential cofactor for the binding of an active-site-directed ligand to PLA2 (Yu et al., 1993). Taken together, the results shown in Figure 2 clearly show that *the large amplitude difference spectrum is a result of binding of a ligand to the active site of the enzyme present at the interface.* MJ72 alone did not produce the spectral change in the absence of the interface, although a solitary EL complex is formed under such conditions (Rogers et al., 1992).

The change in the UV-absorbance induced by the active-site-directed ligand depends on the mole fraction of the ligand. The quantitative aspects of the E*-to-E*L change are not elaborated in this paper. It may, however, be noted that K_L* values obtained by the protection method are similar to those observed with the spectroscopic methods (Jain et al., 1991a,c, 1993; Dupureur et al., 1992a,b). From these values of K_L* it is possible to estimate the proportion of the enzyme in the E* and E*L forms. For example, K_L* for DTPM is 0.03 mol fraction (Jain et al., 1991a), i.e., on DTPM vesicles where its

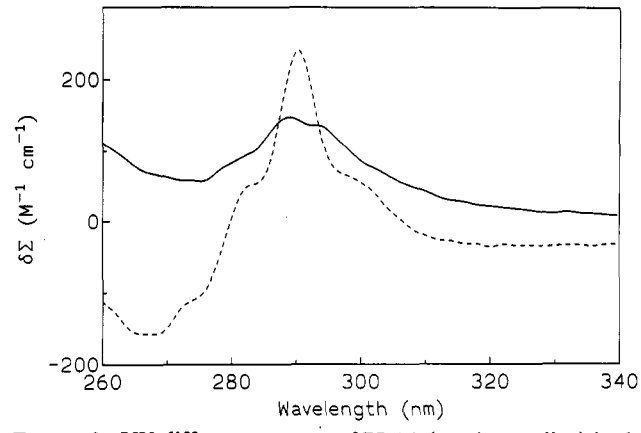

FIGURE 3: UV-difference spectra of PLA2 (continuous line) in the presence of 1 M Na_2SO_4 and (dashed line) in the presence of 3 mM $CaCl_2$ added to the mixture containing 3 mM deoxy-LPC. These experiments were carried out in 10 mM Tris–HCl buffer at pH 8.0 and 23 °C.

mole fraction is 1, essentially all the enzyme in the interface would be in the E*·DTPM form. On the other hand, with dispersions of hexadecylphosphocholine with K_L* = 0.7 mole fraction (Jain et al., 1991c), at saturating bulk amphiphile concentrations about 60% of the bound enzyme would be in the E*L form. These predictions are consistent with the maximum absorbance change at 292 nm observed with hexadecylphosphocholine micelles, which is about 60% of the change observed with DTPM vesicles or with the saturating MJ33 in micelles of the neutral diluent. This is also consistent with the fact that hexadecylphosphocholine is present at the catalytic site in the cocrystals (Tomoo et al., 1992). These results show that quantitative considerations of the equilibria E to E* to E*L are critical for evaluating the structural significance by biophysical studies; otherwise interpretation of such results are compromised due to the presence of more than one species.

The absorbance spectrum of the E form of PLA2 is also sensitive to the binding of other solutes. PLA2 binds with low affinity a second calcium (Pieterson et al., 1974a; Slotboom et al., 1978), polar anions (Hille et al., 1983; Ludescher et al., 1985; Jain et al., 1986b), and monomeric substrate (Pieterson et al., 1974b). The second calcium site involves residues Glu-71 and Ser-72 (Van den Bergh et al., 1989), while anionic ligands interact with the N-terminal region. As shown in Figure 3, the difference spectrum obtained with the E form in the presence of 1 M sulfate has a small positive amplitude (<300 M^{-1} cm^{-1}) with peak and shoulder at about 286 and 294 nm, respectively. Also shown in Figure 3 is the spectrum obtained upon addition of 3 mM calcium to a mixture of PLA2 and deoxy-LPC, which gives a small-amplitude difference spectrum with a peak around 290 nm and shoulders at 280 and 300 nm, which is quite unlike those seen when indole is transferred to a less polar environment (Donovan, 1969). Such low-amplitude spectra from tryptophan arise from H-bonding of indole NH (Strickland et al., 1972) and changes in the ionic environment (Andrews & Forster, 1972). *The similarity of these difference spectra suggests their common origin, i.e., displacement of charged and hydrogen-bonding groups from the vicinity of the indole.* A similar change in the contacts involving charged residues, most likely Ala-1 and Arg-6, also occurs in the E* form of PLA2 as Trp-3 is now immobilized and the segmental motions of the N-terminal and the interfacial binding region are significantly dampened [see anisotropy results described later; also Peters et al. (1992)].

Steady-State Fluorescence Emission Properties of the E, E, and E*L Forms.* The emission maxima, the quantum yields in H_2O and D_2O buffers, the bimolecular quenching constants for succinimide and acrylamide, and the average fluorescence lifetime for the Trp-3 fluorescence from E, E*, and E*L forms are summarized in Table I. The emission maximum of the wild-type PLA2 shifts from 345 (E) to 336 nm on binding to the interface of a neutral diluent (E*) and further to 333 nm for the E*L form. The relative quantum yield of E* is about 2.1, and it increases further to 2.5 for E*L. These relative quantum yields have been corrected for the increase in the absorbance of the E* or E*L at 292 nm. On this scale, the relative quantum yield of NATA is 3.2. A rather low quantum yield of 0.038 suggests that in the E form the fluorescence of Trp-3 is substantially quenched. Some of these quenching processes in the E form are charge-transfer reactions, as seen by the enhanced quantum yields in D_2O. Even though the relative effect is less in the E* form, the absolute magnitude of the D_2O enhancement (a change of 0.2 in the quantum yield) is the same in E and E*. It may be noted that the D_2O effect is observed only in the E and E* forms, whereas in the E*L form the quantum yields (for E*L and E*P) are similar in both H_2O and D_2O [also see Jain et al., (1986b); Jain & Vaz, 1987].

In earlier studies with semisynthetic mutants it was shown that a significant portion of the quenching of Trp-3 fluorescence in E involves interactions with residues Ala-1 and Arg-6 (Van Scharrenburg et al., 1984a; Jain et al., 1986b). Significantly higher quantum yields in E* and E*L forms indicate that some of these quenching contacts are diminished upon binding to the interface. This decrease in the quenching contacts is at least partly due to the loss of motional freedom of Trp-3 in E* and E*L forms (see anisotropy results). From these results it can also be concluded that most of the increase in the fluorescence intensity is associated with the E-to-E* step.

Accessibility of Trp-3 to Quenchers from the Aqueous Phase. As shown in Figure 4, the Stern–Volmer plots for quenching of E, E*, and E*L forms are significantly different. The bimolecular quenching constants for the quenching of the E, E*, and E*P forms of PLA2 by acrylamide and succinimide are summarized in Table I. In the E form, Trp-3 is freely accessible from the aqueous phase, as seen by the magnitude of the k_q values [$(4.5–6.5) \times 10^9$ M^{-1} s^{-1}], which are similar to those seen for NATA and small peptides (Eftink & Ghiron, 1981). These quenching constants for the E form at pH 8.0 compare favorably with earlier reports at pH 6.0 (Ludescher et al., 1985) and confirm our earlier observations with succinimide (Jain & Maliwal, 1985). Compared to that for the E form, in the E* form the quencher accessibility decreased by more than 15-fold in the case of succinimide and about 5-fold in the case of acrylamide. A further 2–3-fold decrease in the accessibility of Trp-3 was seen for the E*L form. Taken together, these quencher accessibility results suggest that Trp-3 is already significantly shielded from the bulk aqueous phase in E*. The observed difference spectrum of E* and the presence of the D_2O effect (Table I), however, show that while Trp-3 in the E* form is shielded from bulk water, the bound water molecules are still present in the microenvironment of Trp-3. This leads to the conclusion that *it is the removal of these bound water molecules during the E*-to-E*L change that gives rise to the characteristic UV difference spectrum and a lack of the D_2O effect.* It may be recalled that in the crystal structure of bovine PLA2 (Dijkstra et al., 1981), eight water molecules are present within 6 Å of Trp-3.

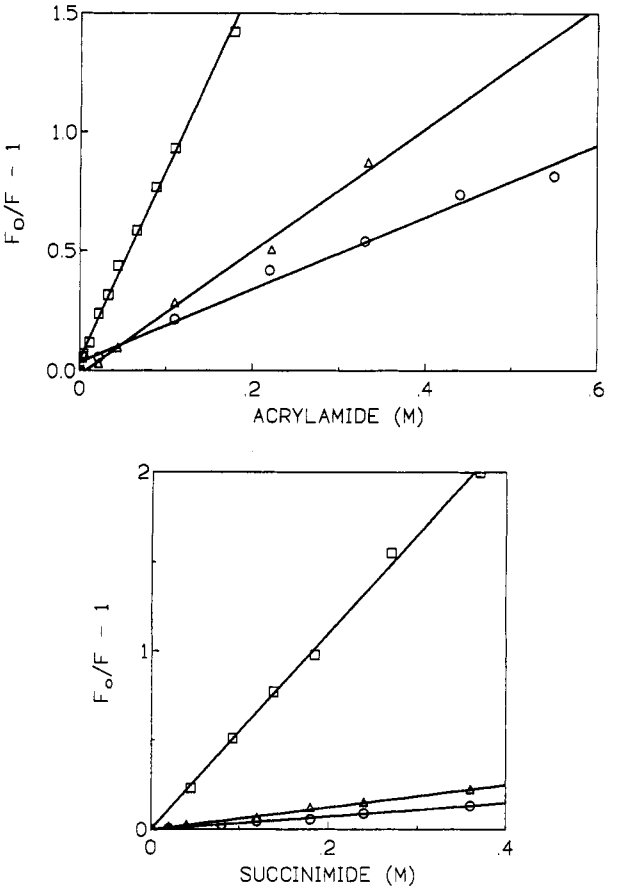

FIGURE 4: Stern–Volmer plots for quenching of the fluorescence emission intensity of (□) PLA2 alone, (△) 3.3 mM deoxy-LPC, and (○) 0.5 mM products of hydrolysis of DMPM by (top) acrylamide and (bottom) succinimide. Other conditions were as in Figure 2.

Fluorescence Lifetimes of the Three Forms of PLA2. Frequency domain measurements of intensity decay from Trp-3 in the three forms of PLA2 are summarized in Table II. The intensity decays of PLA2 in all three forms were significantly heterogeneous and required up to four exponential components to satisfactorily describe the frequency responses. Unfortunately, the presence of four components in the analysis also resulted in the expected high uncertainties in the recovered parameters (Johnson, 1983). The results for the E form with and without calcium and those for the E* and E*L forms were analyzed globally for common exponential decay parameters. The improvement in the χ^2_R in such global analysis between 3 and 4 component was about 3-fold in the case of E and about 1.8-fold in the case of E* and E*L. The confidence limits were calculated at 67% by taking parameter correlations into account (Johnson, 1983). Owing to the complexity in the decays and correlations among the parameters, it may be stressed that it is the trend rather than the absolute values of the fluorescence lifetime components and their amplitudes that are meaningful for the detailed interpretation of tryptophan fluorescence.

As summarized in Table II, the shortest fluorescence lifetime component is around 0.1–0.3 ns, the second component is in the 0.6–1.5-ns range, the third component is between 2.3 and 3.2 ns, and the longest component is around 6–7.5 ns. In the E form, the two shortest fluorescence lifetime components make up about 75% of the fluorescent population, and the longest fluorescence lifetime component makes up less than 6%. In the E* form, a significant increase in the 3-ns component occurs at the expense of the two shortest components, which now make up only about 50% of the fluorescent

Table II: Fluorescence Intensity Decay Parameters of E, E*, and E*L

sample[a]	τ_1 (ns)	τ_2 (ns)	τ_3 (ns)	τ_4 (ns)	α_1	α_2	α_3	α_4	$\langle\tau\rangle$ (ns)	$\chi_R^2(4\tau)$	$\chi_R^2(3\tau)/\chi_R^2(4\tau)$
E(–Ca)	0.11	0.54	2.26	5.73	0.350	0.384	0.206	0.060	1.04	0.53	2.92
	(±0.03)	(±0.06)	(±0.12)	(±0.40)	(±0.054)	(±0.028)	(±0.021)	(±0.008)			
E(+Ca)					0.342	0.411	0.203	0.044	0.98		
					(±0.051)	(±0.028)	(±0.019)	(±0.006)			
E*	0.32	1.59	3.21	7.63	0.277	0.232	0.481	0.009	2.07	0.60	1.80
	(±0.06)	(±0.19)	(±0.15)	(±1.26)	(±0.013)	(±0.042)	(±0.056)	(±0.005)			
E*L(I)					0.199	0.395	0.395	0.011	2.04		
					(±0.015)	(±0.048)	(±0.062)	(±0.006)			
E*L(P)					0.152	0.242	0.604	0.001	2.38		
					(±0.016)	(±0.051)	(±0.064)	(±0.004)			

[a] The E(–Ca) and E(+Ca) were analyzed together. Similarly, the E* and E*L complexes were globally analyzed.

population. In the E*L form, a further shift in the population from the shortest fluorescence lifetime component to the 3.2-ns component is observed. The longest lived component is <1% in the E* and E*L forms. The average fluorescence lifetimes are also summarized in Tables I and II. In the E form, $\langle\tau\rangle$ is about 1.1 ns, which increased to about 2.0–2.1 ns for E* and E*I forms and to 2.4 ns for the E*P form. The trends and the magnitudes of the changes in the average fluorescence lifetime values are similar to those in the quantum yield. These results show that the higher quantum yields of the E* and E*L forms are due to a decrease in the population of the short-lived components and a consequent increase in the population of the 3-ns component. Also, the Trp-3 environment is most heterogeneous in the E forms and least so in the E*L form. Results for the E and E*L forms compare favorably with those observed at pH 6.0 (Ludescher et al., 1985; Kuipers et al., 1991).

The fluorescence lifetime results show that some of the quenching pathways operating in the E form become less significant in the E* and E*L forms. Among the amino acid residues known to quench Trp-3, possible candidates are the protonated amine of Ala-1, the side-chain amide of Gln-4, and the protonated guanidine of Arg-6 (Steiner and Kirby, 1969). Also present in this vicinity are weak quenchers like hydroxyl groups of Ser-7, Thr-70, Ser-72, and Tyr-75 (Lumary and Hershberger, 1978). With Trp-3 becoming immobilized in E* and E*L forms, as seen in anisotropy decays, the quenching contacts present in the E form will be reduced upon binding of the enzyme to the interface. Trp-3 in E*L is, however, still intramolecularly quenched, as indicated by its low quantum yield (0.095) and average fluorescence lifetime (2.4 ns), which are smaller than the values for NATA in water or for the Trp-31 mutant bound to micelles of hexadecylphosphocholine (Kuipers et al., 1991).

Anisotropy Decays in the Three Forms. Results from the frequency domain anisotropy measurements are summarized in Table III, and some representative frequency responses are shown in Figure 5. Anisotropy decay of the E form was satisfactorily described by two correlation times, one for the overall protein motion and the other for local tryptophan motions. The correlation time of about 6 ns represents the overall motion of the protein, while the local motions of Trp-3 in the E form are characterized by a correlation time of 0.1–0.2 ns. The amplitudes associated with the local motions accounted for less than 20% of the limiting anisotropy, indicating that Trp-3 in the E form has significantly restricted motional freedom even though it is exposed on the surface. The motional freedom of Trp-3 and the correlation time of the protein compare favorably with the earlier results obtained at pH 6.0 (Ludescher et al., 1988; Kuipers et al., 1991).

The anisotropy decays of Trp-3 in the bound enzyme could be satisfactorily described by a single correlation time of 18 ns for E* and about 24 ns for E*L forms. As values of the recovered anisotropies of the E* and E*L forms, about 0.275 ± 0.01, are comparable to those observed for frozen tryptophan

Table III: Parameters for Fluorescence Anisotropy Decay of E, E*, and E*L Forms of PLA_2 at 25 °C[a]

sample[a]	r_1	r_2	θ_1 (ns)	θ_2 (ns)	r_0	χ_R^2	$\chi_R^2(\theta)/\chi_R^2(2\theta)$
E	0.060	0.218	0.16	5.7	0.278	0.86	17.36
	(±0.010)	(±0.002)	(±0.04)	(±0.2)	(±0.010)		
E*		0.272		17.5	0.272	0.68	1.20
		(±0.003)		(±0.4)	(±0.003)		
E*L(I)		0.287		23.9	0.287	0.55	1.00
		(±0.003)		(±0.6)	(±0.003)		
E*L(P)		0.267		23.7	0.267	0.72	1.33
		(±0.003)		(±0.7)	(±0.003)		

[a] The excitation wavelength was 298 ± 0.5 nm. The errors are 0.2° in differential phase angles and 0.012 in modulated anisotropies. The amplitude of fast motions in E* and E*L(P) is <0.01 and is ill-determined.

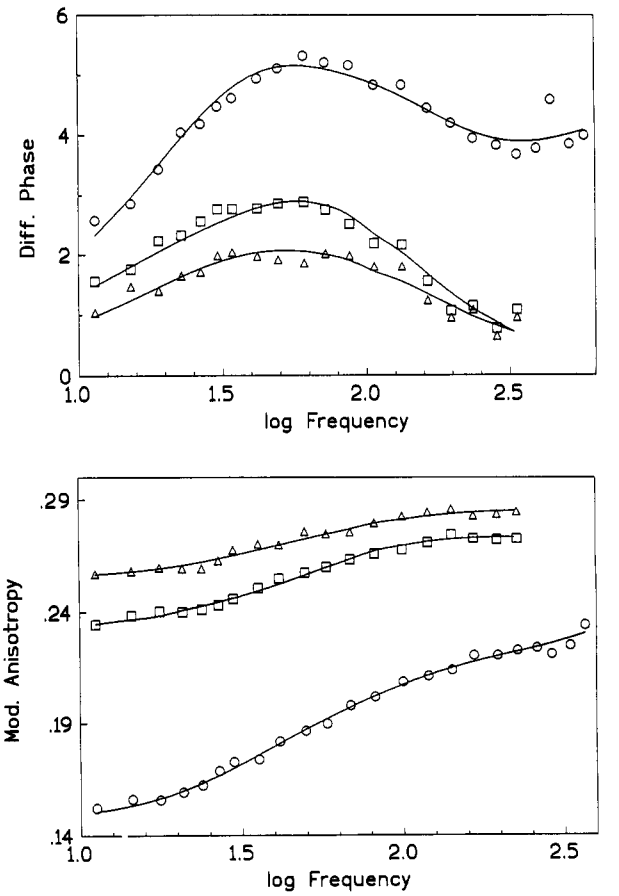

FIGURE 5: Frequency dependence of (top) difference in phase or (bottom) modulated anisotropy of PLA2 in (○) E, (□) E*, and (△) E*L forms at 25 °C. The excitation wavelength was 298 nm.

residue (Valeur & Weber, 1977), all Trp-3 motions are accounted for in these frequency responses. From these results it can be concluded that Trp-3 is essentially immobilized in the E* and the E*L forms of the enzyme. The correlation times of 18 and 24 ns for the E* and E*P forms are, however, significantly smaller than those expected from the size of the micelle–enzyme complex. Smaller than expected correlation times were also observed with the micellar complex of PLA2 with hexadecylphosphocholine (Ludescher et al., 1988; Kuipers et al., 1991). It was suggested that lower than expected correlation times for the enzyme on micelles probably represent an unresolved average of the particle motion and slow isotropic segmental motions. Diffusion of the enzyme around the micelle particle in a few nanoseconds can also result in some depolarization (Ludescher et al., 1988).

DISCUSSION

In the crystal structure of PLA2, the active-site residues including the catalytic residues His-48 and Asp-49 are located in a cavity which is lined with mostly invariant hydrophobic residues. The methyl end of the *sn*-2 chain is in contact with residues 2, 5, and 9 from the (1–12) α-helix (Thunnissen et al., 1990). The collar surrounding the opening of the cavity is made up of several hydrophobic residues, and it in turn is surrounded by a ring of several cationic residues (Ramirez & Jain, 1991). As a part of the interfacial binding region, these residues include not only Trp-3 but also Ala-1, Arg-6, and possibly Lys-10. The N-terminus region is also connected to the loop formed by residues 67–71 (also a part of the interfacial binding region) and the catalytic-site residues His-48 and Asp-99 by a large H-bond network and some bound structural water molecules (Dijkstra et al., 1981, 1983; Thunnissen et al., 1990). Besides their involvement in the binding of PLA2 to the interface, a critical role for several of these residues has also been suggested in the catalytic function (Verheij et al., 1981; Volwerk & de Haas, 1982). As Trp-3 is an integral part of the interfacial binding region, it is not surprising that its spectral properties have been the focus of extensive investigations during the last two decades to characterize the binding of PLA2 to interfaces. Virtually all biophysical studies on the bound PLA2 reported so far (Van Dam-Mieras et al., 1975; Hille et al., 1981; Jain & Maliwal, 1985; Jain et al., 1986b; Ludescher et al., 1985, 1988; Kuipers et al., 1991; Dekker et al., 1991a; Peters et al., 1992) suffer from the limitation that the spectral properties of the E* and E*L forms of PLA2 were not unequivocally resolved. It was so because until recently (Jain et al., 1991a,c) suitable neutral diluents with little affinity for the active site were not identified. In this paper we have characterized the spectral properties of Trp-3 when PLA2 is free (E) and when it is bound to the interface without (E*) or with a ligand at the active site (E*L). We have also attempted to correlate their spectral properties with the crystal structure of PLA2, whose backbone structure is most likely the structure of the active enzyme at the interface (Peters et al., 1992; Scott et al., 1990; Thunnissen et al., 1990).

Studies with the Trp-3-Phe-substituted mutant of PLA2 showed that the absorption and fluorescence properties reported here are primarily due to Trp-3 with only minor contribution from the tyrosine residues [results not shown; see also Van Dam-Mieras et al. (1975)]. Trp-3 is present on the surface, and in the E form it is highly accessible to aqueous quenchers. Surprisingly, however, the anisotropy decays suggest highly restricted motional freedom for both Trp-3 and the N-terminus. The origin of such remarkable restrictions on the motional freedom of Trp-3 and the N-terminus in the E form is most likely in the hydrogen-bonding network involving Ala-1, Gln-4, Tyr-69, and Glu-71 residues, which form part of the interfacial binding region, and in the polar interactions of the indole ring with bound water molecules (Dijkstra et al., 1981, 1983; Axelson et al., 1991). The role of the hydrogen-bonding network in restricting Trp-3 mobility and most likely the mobility of the N-terminus was suggested by the significantly different behavior of a mutant in which Leu-31 was replaced by Trp. The residue 31, like Trp-3, is part of the interfacial recognition region and is fully exposed to the bulk water (Thunnissen et al., 1990).

Significant changes in the spectroscopic properties of Trp-3 were observed upon binding of PLA2 to the micellar interface of the neutral diluent. In the E* form, both the fluorescence intensity and the average fluorescence lifetimes were almost 2-fold higher than that for the E form. It may be noted that most of the increase in the fluorescence quantum yield upon binding to the interface was associated with the E-to-E* step. The origin of this fluorescence increase upon the formation of the E* form also lies in the presence of the quenching residues such as α-NH_3^+ of Ala-1, protonated guanidinium of Arg-6, and hydroxylic groups of serines and tyrosines. Since these groups are inefficient quenchers (Steiner & Kirby, 1969), they are probably in near-direct contact with the indole ring. In the light of such a complex quenching environment, it is not surprising that Trp-3 of PLA2 has a rather low quantum yield and shows highly heterogeneous intensity decays. Thus the explanation for increased quantum yields of E* forms would be that some of the quenching contacts of Trp-3 which are in the E form are diminished due to both dampening of the segmental motions and conformational adjustments of the N-terminus due to the interfacial contacts. The dampening of the limited motional freedom of Trp-3 at the interface also suggests significant tryptophan–protein matrix interactions in the E* form.

A remarkable decrease in the accessibility of Trp-3 to the aqueous quenchers was also observed in the E* form. This suggests that the interfacial binding region is in contact with the micelle of the neutral diluent and therefore shielded from the aqueous phase. Surprisingly, some D_2O effect is still observed in the E* form. Together with the small amplitude of the difference spectrum, these results indicate that the microenvironment of E* is still highly polar. *These observations, therefore, suggest that the interfacial region of E*, although shielded from the bulk solvent, is still solvated.* The similarity in the absorption difference spectra of the E* form and that observed with binding of sulfate to the E form suggests that one of the events associated with the E-to-E* step is separation of Trp-3 from some of the charge groups present in its microenvironment.

Formation of E*L from E* further increases the quantum yield as well as the average fluorescence lifetime, while Trp-3 becomes somewhat more shielded from the aqueous quenchers. There was further dampening of the motional freedom of Trp-3 and quite possibly of the N-terminal region. Trp-3 in E*L is in a less polar environment, as indicated by the amplitude of the difference spectrum and by the D_2O effect. Together, *these results suggest that one of the effects of occupancy of the active site of E* is removal of water molecules from the microinterface between the enzyme and the interface.* Such a coupling between the two events has an important bearing both on the processivity of interfacial catalysis, as it would greatly facilitate transfer of phospholipid molecules from the interface to the active site of the enzyme at the interface (Jain et al., 1986a,c, 1988; Jain & Vaz, 1987), and also on the

possible mechanism of interfacial activation (Jain et al., 1993).

The remarkable heterogeneity in Trp-3 fluorescence intensity decays in both the E* and E*L forms, even though the N-terminal segmental motions are significantly dampened, is indicative of the presence of conformational heterogeneity. It may be noted that both the restrained molecular dynamics calculations (Sessions et al., 1988; Gross et al., 1990) and a multidimensional NMR study of the E form (Dekker et al., 1991a,b) indicate considerable segmental mobility in the interfacial binding region including the N-terminus. Similarly, dampening of N-terminal segmental motion has been observed by NMR for E*I in micelles (Peters et al., 1992).

To recapitulate, on the basis of the weight of the evidence, we suggest that *for PLA2 bound to the interface, the N-terminal region and the associated interfacial binding region are an ensemble of conformations* rather than a discrete conformational state. It may be argued that such an ensemble of readily interchangeable conformers with a low-energy barrier would be more effective in accommodating diverse molecular, structural, and organizational features of the interface that PLA2 may encounter on aggregates of different composition. Beyond the changes in the orientations and contacts of the specific amino acid residues as necessitated by the contact of PLA2 with the lipid–water interface, changes in the solvation characteristics of the active site and the interfacial binding region must also occur during the E*-to-E*L change. Such changes are key to understanding interfacial equilibrium and catalytic processes. The hydrophobic character of the interfacial binding region of PLA2 would also promote the ordering of the water molecules when in solution (the E form), as is evident in the crystal structure of the enzyme. Therefore, *it appears that at the functional level a major change in the solvation of the interface and the active site is triggered by the binding of a ligand to the active site.* The desolvation process is likely to be driven by the headgroup interactions at the active site and by the hydrophobic effect from the fatty acid chains. Therefore, the ligand substitution of the water molecules bound to the calcium ion at the active site could also possibly trigger successive removal of the water molecules from the active site as well as from the interfacial binding region as necessitated for the interactions with the local structural and organizational features of the interface.

REFERENCES

Alcala, J. R., Gratton, E., & Prendergast, F. G. (1987) *Biophys. J. 51*, 925–936.

Andrews, L. J., & Forster, L. S. (1972) *Biochemistry 11*, 1875–1879.

Axelson, P. H., Gratton, E., & Prendergast, F. G. (1991) *Biochemistry 30*, 1173–1179.

Berg, O. G., Yu, B.-Z., Rogers, J., & Jain, M. K. (1991) *Biochemistry 30*, 7283–7297.

Dekker, N., Peters, A. R., Slotboom, A. J., Boelens, R., Kaptein, R., Dijkman, R., & de Haas, G. H. (1991a) *Eur. J. Biochem. 199*, 601–607.

Dekker, N., Peters, A. R., Slotboom, A. J., Boelens, R., Kaptein, R., & de Haas, G. H. (1991b) *Biochemistry 30*, 3135–3147.

Dijkstra, B. W., Kalk, K. H., Hol, W. G. J., & Drenth, J. (1981) *J. Mol. Biol. 147*, 97–123.

Dijkstra, B. W., Renetseder, R., Kalk, K. H., Hol, W. G. J., & Drenth, J. (1983) *J. Mol. Biol. 168*, 163–179.

Donovan, J. W. (1969) in *Physical Principles and Techniques of Protein Chemistry* (Leach, S. J., Ed.) Part A, pp 101–170, Academic Press, New York.

Dupureur, C. M., Yu, B.-Z., Jain, M. K., Noel, J. P., Deng, T., Li, Y., Byeon, I. L., & Tsai, M. D. (1992a) *Biochemistry 31*, 6402–6413.

Dupureur, C. M., Yu, B.-Z., Mamone, J. A., Jain, M. K., & Tsai, M. D. (1992b) *Biochemistry 31*, 10576–10583.

Eftink, M. R., & Ghiron, C. A. (1981) *Anal. Biochem. 114*, 199–227.

Gros, P., van Gunstern, W. F., & Hol, W. G. J. (1990) *Science 249*, 1149–1152.

Hille, J. D. R., Donne-Op den Kelder, G. M., Sauve, P., de Haas, G. H., & Egmond, M. R. (1981) *Biochemistry 20*, 4068–4073.

Hille, J. D. R., Egmond, M. R., Dijkman, R., Van Oort, M. G., Jirgensons, B., & de Haas, G. H. (1983) *Biochemistry 22*, 5347–5353.

Jain, M. K., & Maliwal, B. P. (1985) *Biochim. Biophys. Acta 814*, 134–140.

Jain, M. K., & Vaz, W. L. C. (1987) *Biochim. Biophys. Acta 905*, 1–8.

Jain, M. K., & Berg, O. G. (1989) *Biochim. Biophys. Acta 1002*, 127–156.

Jain, M. K., Egmond, M. R., Verheij, H. M., Apitz-Castro, R. J., Dijkman, R., & de Haas, G. H. (1982) *Biochim. Biophys. Acta 688*, 341–348.

Jain, M. K., Rogers, J., Jahagirdar, D. V., Marecek, J. F., & Ramirez, F. (1986a) *Biochim. Biophys. Acta 860*, 435–447.

Jain, M. K., Maliwal, B. P., de Haas, G. H., & Slotboom, A. J. (1986b) *Biochim. Biophys. Acta 860*, 448–461.

Jain, M. K., de Haas, G. H., Marecek, J. F., & Ramirez, F. (1986c) *Biochim. Biophys. Acta 860*, 475–483.

Jain, M. K., Rogers, J., & de Haas, G. H. (1988) *Biochim. Biophys. Acta 940*, 51–62.

Jain, M. K., Yu, B.-Z., Rogers, J., Ranadive, G. N., & Berg, O. G. (1991a) *Biochemistry 30*, 7306–7317.

Jain, M. K., Ranadive, G. N., Yu, B.-Z., & Verheij, H. M. (1991b) *Biochemistry 30*, 7330–7340.

Jain, M. K., Tao, W., Rogers, J., Arenson, C., Eibl, H., & Yu, B.-Z. (1991c) *Biochemistry 30*, 10256–10268.

Jain, M. K., Yu, B.-Z., & Berg, O. G. (1993) *Biochemistry* (in press).

Johnson, M. L. (1983) *Biophys. J. 44*, 101–106.

Kuipers, O. P., Vincent, M., Brochon, J.-C., Verheij, H. M., de Haas, G. H., & Gallay, J. C. (1991) *Biochemistry 30*, 8771–8785.

Laczko, G., Gryczynski, I., Gryczynski, Z., Wiczk, W., Malak, H., & Lakowicz, J. R. (1990) *Rev. Sci. Instrum. 61*, 2331–2337.

Lakowicz, J. R., Laczko, G., Cherek, H., Gratton, E., & Limkeman, M. (1984) *Biophys. J. 46*, 463–477.

Ludescher, R. D., Volwerk, J. J., de Haas, G. H., & Hudson, B. S. (1985) *Biochemistry 24*, 7240–7249.

Ludescher, R. D., Johnson, I. D., Volwerk, J. J., de Haas, G. H., Jost, P. C., & Hudson, B. S. (1988) *Biochemistry 27*, 6618–6628.

Lumry, R., & Hershberger, M. (1978) *Photochem. Photobiol. 27*, 819–840.

Maliwal, B. P., & Lakowicz, J. R. (1986) *Biochim. Biophys. Acta 873*, 161–172.

Meijer, H., Puijk, W. C., Dijkman, R., Foda-van der Hoorn, M. M. E. L., Pattus, F., Slotboom, A. J., & de Haas, G. H. (1979) *Biochemistry 18*, 3589–3597.

Noel, J. P., Bingham, C. A., Deng, T., Dupureur, C. M., Hamilton, K. J., Jiang, R.-T., Kwak, J.-G., Secharudu, C., Sundaralingam, M., & Tsai, M. D. (1991) *Biochemistry 30*, 11801–11811.

Peters, A. R., Dekker, N., Van den Berg, L., Boelens, R., Kaptein, R., Slotboom, A. J., & de Haas, G. H. (1992) *Biochemistry 31*, 10024–10030.

Pieterson, W. A., Volwerk, J. J., & de Haas, G. H. (1974a) *Biochemistry 13*, 1439–1455.

Pieterson, W. A., Vidal, J. C., Volwerk, J. J., & de Haas, G. H. (1974b) *Biochemistry 13*, 1455–1460.

Ramirez, F., & Jain, M. K. (1991) *Proteins 9*, 229–239.

Rogers, J. R., Yu, B.-Z., & Jain, M. K. (1992) *Biochemistry 31*, 6056–6062.
Scott, D. L., White, S. P., Otwinowski, Z., Gelb, M. H., & Sigler, P. B. (1990) *Science 250*, 1563–1566.
Sessions, R. B., Dauber-Osgnthorpe, P., & Osgnthorpe, D. J. (1988) *J. Mol. Biol. 209*, 617–633.
Slotboom, A. J., Jensen, E. H. J. M., Vlijm, H., Pattus, E., Soares de Araujo, P., & de Haas, G. H. (1978) *Biochemistry 17*, 4593–4600.
Steiner, R. F., & Kirby, E. P. (1969) *J. Phys. Chem. 73*, 4130–4135.
Strickland, E. H., Billups, C., & Kay, E. (1972) *Biochemistry 11*, 3657–3662.
Thunnissen, M. M. G. M., Ab, E., Kalk, K. H., Drenth, J., Dijkstra, B. W., Kuipers, O. P., Dijkman, R., de Haas, G. H., & Verheij, H. M. (1990) *Nature 347*, 689–691.
Tomoo, K., Ohnish, H., Doi, M., Ishida, T., Inoue, M., Ikeda, K., & Mizuno, H. (1992) *Biochem. Biophys. Res. Commun. 187*, 821–827.
Valeur, B., & Weber, G. (1977) *Photochem. Photobiol. 25*, 441–444.
Van Dam-Mieras, M. C. E., Slotboom, A. J., Pieterson, W. A., & de Haas, G. H. (1975) *Biochemistry 14*, 5387–5394.
Van den Bergh, C. J., Bekkers, A. C. P. A., Verheij, H. M., & de Haas, G. H. (1989) *Eur. J. Biochem. 182*, 307–313.
Van Scharrenburg, G. J. M., Jansen, E. H. J. M., Egmond, M. R., de Haas, G. H., & Slotboom, A. J. (1984a) *Biochemistry 23*, 6285–6294.
Van Scharrenburg, G. J. M., Puijk, W. C., Seeger, P. R., de Haas, G. H., & Slotboom, A. J. (1984b) *Biochemistry 23*, 1256–1263.
Van Scharrenburg, G. J. M., Slotboom, A. J., de Haas, G. H., Mulqueen, P., Breen, P. J., & Horrocks, W. W. (1985) *Biochemistry 24*, 334–339.
Verheij, H. M., Slotboom, A. J., & de Haas, G. H. (1981) *Rev. Physiol. Biochem. Pharmacol. 91*, 91–203.
Volwerk, J. J., & de Haas, G. H. (1982) in *Lipid Protein Interactions* (Jost, P. C., & Griffith, O. H., Eds.) Vol. 1, pp 69–149, John Wiley & Sons, New York.
Weber, G. (1977) *J. Chem. Phys. 66*, 4081–4091.
Yu, B.-Z., Berg, O. G., & Jain, M. K. (1993) *Biochemistry 32*, 6485–6492.